Genomic basis of drought resistance in *Fagus sylvatica*

Markus Pfenninger[1,2,3], Friederike Reuss[1], Angelika Kiebler[1], Philipp Schönnenbeck[4], Cosima Caliendo[1,4], Susanne Gerber[4], Berardino Cocchiararo[3,5], Sabrina Reuter[6], Nico Blüthgen[6], Karsten Mody[6,11], Bagdevi Mishra[7], Miklós Bálint[3,8,9], Marco Thines[3,7,10], Barbara Feldmeyer[1]

[1] Molecular Ecology, Senckenberg Biodiversity and Climate Research Centre, Frankfurt am Main, Germany

[2] Institute for Organismic and Molecular Evolution, Johannes Gutenberg University, Mainz, Germany

[3] LOEWE Centre for Translational Biodiversity Genomics, Frankfurt am Main, Germany

[4] Institute of Human Genetics, University Medical Center, Johannes Gutenberg University, Mainz, Germany

[5] Conservation Genetics Section, Senckenberg Research Institute and Natural History Museum Frankfurt, Gelnhausen, Germany

[6] Ecological Networks lab, Department of Biology, Technische Universität Darmstadt, Darmstadt, Germany

[7] Biological Archives, Senckenberg Biodiversity and Climate Research Centre, Frankfurt am Main, Germany

[8] Functional Environmental Genomics, Senckenberg Biodiversity and Climate Research Centre, Frankfurt am Main, Germany

[9] Agricultural Sciences, Nutritional Sciences, and Environmental Management, Universität Giessen, Giessen, Germany

[10] Institute for Ecology, Evolution and Diversity, Johann Wolfgang Goethe-University, Frankfurt am Main, Germany

[11] Department of Applied Ecology, Hochschule Geisenheim University, Geisenheim, Germany

Abstract

In the course of global climate change, central Europe is experiencing more frequent and prolonged periods of drought. The drought years 2018 and 2019 affected European beeches (*Fagus sylvatica* L.) differently: even in the same stand, drought damaged trees neighboured healthy trees, suggesting that the genotype rather than the environment was responsible for this conspicuous pattern. We used this natural experiment to study the genomic basis of drought resistance with Pool-GWAS. Contrasting the extreme phenotypes identified 106 significantly associated SNPs throughout the genome. Most annotated genes with associated SNPs (>70%) were previously implicated in the drought reaction of plants. Non-synonymous substitutions led either to a functional amino acid exchange or premature termination. A SNP-assay with 70 loci allowed predicting drought phenotype

in 98.6% of a validation sample of 92 trees. Drought resistance in European beech is a moderately polygenic trait that should respond well to natural selection, selective management, and breeding.

Keywords

Genome-wide association study, genomic prediction, forest tree, Fagales, conservation genomics, functional environmental genomics

Impact Statement

European beech harbours substantial genetic variation at genomic loci associated with drought resistance and the loci identified in this study can help to accelerate and monitor adaptation to climate change.

Introduction

Climate change comes in many different facets, amongst which are prolonged drought periods (Christensen *et al.* 2007). The Central European droughts in the years 2018 and 2019 caused severe water stress in many forest tree species, leading to the die-off of many trees (Schuldt *et al.* 2020a). Among the suffering tree species was European beech, *Fagus sylvatica* L. As one of the most common deciduous tree species in Central Europe, *F. sylvatica* is of great ecological importance: beech forests are a habitat for more than 6,000 different animal and plant species (Brunet *et al.* 2010; Dorow *et al.* 2010). The forestry use of beech in 2017 generated a turnover of more than 1 billion € in Germany alone (Thünen_Institute 2020), without taking the economic and societal value of the ecosystem services of woods into account (Elsasser *et al.* 2016). However, the drought years 2018 and 2019 severely impacted the beech trees in Germany (Paar & Dammann 2019). Official reports on drought damage in beech recorded 62% of trees with rolled leaves and 20-30% of small leaves, mainly in the crown, resulting in 7% of badly damaged or dead trees. As shown before (Bressem 2008), most trees affected by drought stress were medium to old aged.

Under favourable conditions, beech is a competitive and shade tolerant tree species, dominating mixed stands (Pretzsch *et al.* 2013). High genetic diversity within populations supports adaptation to local conditions (Kreyling *et al.* 2012). Significant differences between local populations in tolerance to various stress factors such as early frost (Czajkowski & Bolte 2006), drought (Cocozza *et al.* 2016; Harter *et al.* 2015) or air pollution (Müller-Starck 1985) are known. The distribution of *F. sylvatica* is mainly limited by water-availability, as the tree does not tolerate particularly wet or dry conditions (Sutmöller *et al.* 2008). Therefore, it is quite conceivable that the species could suffer even more under the predicted future climatic conditions than today (Sutmöller *et al.* 2008).

Despite the widespread, severe drought damage, a pattern observed in all beech forests was very noticeable (personal observations). Using crown deteriation as significant indicator for drought damage (Choat *et al.* 2018), not all trees in a beech stand were equally damaged or healthy. The damage occurred rather in a mosaic-like pattern instead. Even though the extent of drought damage varied among sites, apparently completely healthy trees immediately neighboured severely damaged ones and *vice versa*. This observation gave rise to the hypothesis that not the local environmental conditions might be decisive for the observed drought damage, but rather the genetic make-up of the individual trees.

We decided to draw on this natural “experimental set-up” to infer the genomic basis underlying the drought susceptibility in *F. sylvatica*. We identified more than 200 neighbouring pairs of trees with extreme phenotypes and used a Pool-GWAS approach (Bastide *et al.* 2013) to infer associated SNP loci by contrasting allele frequencies with replicated pools of drought susceptible and resistant individuals. In addition, we individually re-sequenced a subset of 51 pairs of susceptible and resistant trees. If the observed pattern indeed has a genetic basis, identifying the associated loci would enable

the genomic prediction of drought resistance (Stocks *et al.* 2019). Constructing a SNP assay from the most highly phenotype associated SNPs, we validated 70 identified loci by predicting the drought phenotype of an additional set of beech trees from their genotype at these loci using Linear Discriminant Analysis and a new Machine Learning approach (Horenko 2020). These accurate genomic prediction tools, e.g., the choice of drought resistant seed producing trees and selective logging could help accelerate and monitor natural selection and thus harness beech forests against climate change (Waldvogel *et al.* 2020).

Results

Sampling, climate development and phenotyping

Damaged and healthy beech tree pairs were sampled from woods in the lowland Rhein-Main plain, the adjacent low mountain ranges of Odenwald and Taunus, and mountain ranges from Central and Northern Hessen (Fig. 1A). When summarising the climatic conditions from 1950 to 2019 for the sampling sites in a principal component analysis (PCA), the sites were divided into two groups by axis 1, a temperature gradient. The Taunus mountain sites grouped with those from the northern part of Hessen, while the Rhein-Main plain clustered with the Odenwald sites (Fig. 1B). This grouping was also used to construct the GWAS pools (see below). Comparing the climate from the 1950s, when most of the trees sampled were already in place, with the decade from 2010-2019, showed that all local conditions changed substantially and similarly in the direction and extent of warmer and drier conditions (Fig. 1B). The steepest temperature increase occurred in the 1980s, while precipitation patterns mainly changed in the last decade (Suppl. Fig. 1). A wide range of parameters, potentially relevant as selection pressures changed drastically during this period: the mean January daily minimum temperature at the sampling sites increased by 1.49°C from -2.64°C (s.d. 1.68°C) in the 1950s to -1.15°C (s.d. 2.50°C) during the last decade. The mean August daily maximum temperatures increased even more by 2.37°C from 22.06°C (s.d. 1.95°C) to 24.43°C (s.d. 2.35°C). Simultaneously, mean annual precipitation decreased by 40.5 mm or 5.5% from 741.2 mm (s.d. 85.8 mm) to 700.7 mm (s.d. 70.9 mm). Most of the precipitation loss (84%) occurred during the main growth period between April and September, with a decrease of 33.9 mm from 410.4 mm (s.d. 36.1 mm) to 376.5 mm (s.d. 25.6 mm).

Mean monthly evaporation potential, available from 1991 onwards, showed that, compared to the beginning of the 1990s, the main growth period of beech from April to September became increasingly drier, with up to 30 mm more evaporation per month. The drought dynamics suggested that the years 2018 and 2019 were not outliers, but rather part of a long-term, accelerating trend (Fig. 1C), following the overall global pattern (Büntgen *et al.* 2021; Trenberth *et al.* 2014).

There was a strong negative correlation (r = 0.695) between the drought strength during the main growth period (Apr- Sept) and a proxy for (green) leaf cover (leaf area index, LAI) for the sampled plots in the years 2015-2019 (Suppl. Fig. 2). This observation suggested that leaf loss and dried leaves are good indicators for drought stress.

The mean distance between paired trees was 5.1 m (s.d. 3.4 m, Suppl. Fig. 3). Phenotypic measurements generally confirmed the study design and selection of trees: healthy and damaged trees within each tree pair did not differ significantly in *trunk circumference*, *tree height*, *canopy closure* and *competition index* (Fig. 2 A-D, Suppl. Table 2). Hence, these parameters were not considered in further analyses. As expected, and confirming the assignment of damage status, the quantity of *dried leaves* and *leaf loss* differed substantially between damaged and healthy ones (Fig. 2 E-F, Suppl. Table 2). A sample of photographs contrasting damaged and healthy paired trees can be found in the Suppl. Fig. 4.

128 *Linkage disequilibrium, population structure and genome-wide association study*

129 For a subsample of 300 out of the 402 sampled beech trees we generated four DNA pools from two
130 climatically distinct regions (North and South Hessen, Fig. 1B), contrasting trees that were either
131 healthy or highly drought damaged respectively (Tab. S1). The "South" pools consisted of 100
132 individuals each, whereas the "North" pools contained 50 individuals each. We created ~50GB 150
133 bp-paired end reads with insert size 250-300 bp on an Illumina HiSeq 4000 system per pool. More
134 than 96% of the reads mapped against the repeat-masked chromosome level beech reference
135 genome (accession no. PRJNA450822). After filtering the alignment for quality and a coverage
136 between 15x and 70x, and removing indels, allele frequencies for 9.6 million SNPs were scored. All
137 100 individuals from the North population were additionally individually re-sequenced to ~20x
138 coverage each (for more details see M&M). This data was used to a) determine individual variability
139 in allele frequencies and b) to validate the information content of the candidate SNP-set.

140 Using all individually resequenced individuals, we inferred the extent of genome wide linkage
141 disequilibrium (LD;). The plot of LD r^2 against the distance from the focal SNP showed that LD fell to
142 $r^2 \sim 0.3$ within less than 120 bp, which means that genome positions such a distance apart are on
143 average effectively unlinked (Fig. 3A). The PCA on SNP variation of the individually re-sequenced
144 trees from the North population explained 12.3% of accumulated variation on the first two axes (Fig.
145 3B). Trees from the same sampling site (within the North population) did not tend to cluster together
146 (Fig. 3B). F_{ST} estimates among pools for non-overlapping 1 kb windows were virtually identical among
147 healthy/damaged pools within region as compared to between regions (Suppl. Fig. 5). Trees within a
148 phenotypic class were genomically not more similar than between classes (Suppl. Fig. 6, ANOSIM R =
149 -0.008, p = 0.76, 9,999 permutations).

150 Pool-GWAS analysis identified 106 SNPs significantly associated with the drought damage status
151 using a Cochran-Mantel-Haenszel test on the two pairs of damaged and healthy pools after false
152 discovery rate correction and a cut-off at 1×10^{-2} (Fig. 4A, Suppl. Fig. 7). Some of the 106 SNPs were
153 in close physical proximity (<120bp) and thus probably linked. Taking this into account, 80
154 independent genomic regions were associated with the drought damage status. None of the
155 significantly differentiated SNP loci was mutually fixed; the observed allele frequency differences
156 between healthy and damaged trees at associated loci ranged between 0.12 and 0.51 (Fig. 4B).

157 *Associated genes and gene function*

158 Of the 106 significant SNPs, 24 were found in 20 protein coding genes (Table 1). Forty-nine genes
159 were the closest genes to the remaining 82 SNPs. For 61 of these genes, the best BLAST hit was with
160 a tree, mainly from the Fagales genera *Quercus* and *Castanea* (Table 1, Suppl. Table 3). Among the 24
161 SNPs in genes, we observed 13 non-synonymous changes. In eleven of these changes, the alternate
162 allele was associated with the damaged phenotype and only in two cases with the healthy
163 phenotype. Three of the non-synonymous substitutions resulted in a stop codon. Of the remaining
164 ten, eight exchanges caused a major change in amino acid characteristics and thus probably in
165 protein folding or function (Table 1). One gene, a PB1 domain-containing protein tyrosine kinase,
166 contained four non-synonymous changes, suggesting that the allele version associated with the
167 damaged phenotype lost its function (Tab. 1). From the 20 genes with significant SNPs, functional
168 information could be obtained from the UniProt database for 14 (Suppl. Table 3). Of these, ten genes
169 were associated in previous studies with either environmental stress response (two) or specifically
170 with drought stress response (eight; Suppl. Table 3). Of the 49 predicted genes closest to the
171 remaining significant SNPs (Tab. 1), 16 could be reliably annotated (Suppl. Table 2). Twelve had been
172 directly related to drought in previous studies, while three were previously associated with other
173 environmental stress responses (Suppl. Tab. 3).

Genomic prediction

We furthermore set out to determine how many SNPs were needed to successfully predict the drought susceptibility of individual trees, i.e. to develop a genotyping assay. All Pool-GWAS SNPs in addition to the top 20 individual re-sequencing SNPs were used to create a SNP combination to reach a genotyping success threshold of min. 90%. After excluding loci due to technical reasons and filtering for genotyping success, seventy loci proved to be suitable for reliable genotyping with a SNP assay. We genotyped only individuals sampled in 2019 that were not used to identify the SNPs in the first place plus paired individuals sampled in Aug 2020. On average, each of the 95 individuals was successfully genotyped at 67.7 loci (96.7%). We coded the genotypes as *0* for homozygous reference allele, *1* for heterozygous and *2* for the homozygous alternate allele, thus assuming a linear effect relationship. Figure 5 shows the genotypogram for the tested individuals.

Linear discriminant analysis (LDA) correctly predicted the observed phenotype from the genotype in 91 of 92 cases (98.9%). Prediction success decreased to 65% when successively removing loci from the analysis (Suppl. Fig. 8). Nevertheless, ordering the individuals according to the LDA score of axis 1 revealed no clear genotype pattern that distinguished healthy from damaged trees (Fig. 5). Observed heterozygosity at loci used in the SNP assay of individuals in the upper half of predictive values for a healthy phenotype was not significantly different from heterozygosity of the lower half (Suppl. Fig. 9). Ordering the loci according to their squared loadings showed that loci's contribution to the genomic prediction differed substantially (Fig. 5). As expected, the histogram of LDA scores showed two peaks, corresponding to the two phenotypes (Suppl. Fig. 10).

To validate the results of the LDA prediction and to circumvent potential overfitting due to the small sample size, we also applied a non-parametric Machine Learning algorithm for feature selection and clustering that was especially designed for small sample sizes (Gerber2020, Horenko2020). The Method identified the 20 most-significant SNPs allowing to make an almost 85% correct classification that distinguished healthy from damaged trees (Suppl. Table 5).

Discussion

Over the last two decades, increasing drought periods caused severe damage to European forests (Schuldt *et al.* 2020b; Etzold *et al.* 2019; Pretzsch *et al.* 2013). Conifers seem to suffer the most, but also deciduous trees were strongly affected (Schuldt *et al.* 2020b). Weather data from our study area from 1950 onwards suggested that the climatic conditions for beech trees in the area investigated changed dramatically during this period. Roughly estimating the tree age from their trunk circumference (Bošeľa *et al.* 2014), more than a third of the trees were already in place at the beginning of this period. About 60% were recruited prior to the acceleration of temperature change from the 1980s onwards. As a result, trees in the mountainous regions of the study area today experience climatic conditions comparable to those experienced by low land trees in the 1950s, which in turn now experience a climate that used to be typical for regions much further South. Given the documented propensity of beech for local adaptation (Gárate-Escamilla *et al.* 2019; Pluess *et al.* 2016; Aranda *et al.* 2015), including drought (Bolte *et al.* 2016), it is therefore conceivable that current conditions exceed the reaction norm of some previously locally well-adapted genotypes with detrimental consequences for their fitness. If the trend of an increasingly drier vegetation period persists, this will likely affect an even larger proportion of the currently growing beeches.

Evolutionary genomics will be indispensable to predict and manage the impact of global change on biodiversity (Waldvogel *et al.* 2020). As already shown for other partially managed (tree) species (Stocks *et al.* 2019), in particular pool-GWAS approaches (Endler *et al.* 2016) have proven to be useful in guiding conservation management.

Our strictly pairwise sampling design avoided many pitfalls of GWAS studies, arising, e.g., from cryptic population structure and shared ancestry (Hoban *et al.* 2016; Wellenreuther & Hansson 2016). Despite presented evidence from this and other studies (Schuldt et al. 2020) that the observed crown damages in large parts of Central Europe used for phenotyping here are directly or indirectly due to the severe drought years 2018 and 2019, we must acknowledge that we have no direct physiological proof that the trees surveyed here indeed suffered from drought stress. In addition, the observed diagnostic symptoms are not specific to drought stress. Nevertheless, an unknown independent stressor would have needed to accidentally co-occur spatially and temporally with the drought. The phenotypical drought response of individual trees may also be influenced by microspatial variation (Carrière *et al.* 2020). In the present study, however, the mean distance between sampled paired trees of about 5 m assured that their roots systems largely overlapped. Thus, environmental variation in soil quality, rooting depth, water availability or other factors should have been minimal. Please note that any phenotypical misclassification due to such microspatial differences would have rather dissimulated the genotypic differences found in GWAS than enhanced them artificially. Also he lumping of similar phenotypes induced by different stressors is unlikely to have the same genomic basis and resulting in significant GWAs results.

As expected from previous studies (Rajendra *et al.* 2014), we found no population structure among the sampling sites. Applying relatively strict significance thresholds, we found systematic genomic differences between the healthy and damaged trees. In all cases, these differences were quantitative and not categorical, i.e. we found allele frequency changes but no fixed SNPs between phenotypes. Significant SNPs were mostly not clustered - we found on average 1.4 selected SNPs in a particular region. These findings were in line with the observed very short average LD in *F. sylvatica,* indicating that polymorphisms associated with the two phenotypes were likely old standing genetic variation (Harris & Nielsen 2013). Moreover, such SNPs are mostly detached from the background in which they arose And they are therefore often the actual causal variants. This observation is underlined by the high proportion of non-synonymous significant SNPs within genes, which in most cases caused substitution to amino acid with different properties or even premature termination. Such deviant variants with likely substantial functional or conformational changes in the resulting proteins may be selectively neutral or nearly neutral under ancestral benign conditions, but may become selectively relevant under changing conditions (Paabi & Rockman 2014). Interestingly, most of the allelic variants associated with a healthy phenotype were also the variants in the reference genome. This might be due to the choice of the *F. sylvatica* individual from which the reference genome was gained (Mishra *et al.* 2018). This more than 300-year-old individual is standing at a particularly dry site on a rocky outcrop on the rim of a scarp where precipitation swiftly runs off. Trees at such sites were likely selected for drought tolerance.

Even though the area sampled for this study was limited relative to the species distribution range, it comprised its core area. In addition, the climatic variation covered by the sampling sites for this study is representative for large parts of the species range (Baumbach *et al.* 2019). The relatively limited population structure over large parts of the species range (Magri *et al.* 2006) together with the propensity for long range gene- flow (Belmonte *et al.* 2008) suggested that the genomic variation responsible for drought tolerance identified here is widely distributed (Lander *et al.* 2021). Nevertheless, an assessment of the geographic distribution of the drought related genomic variants over the entire distribution range would yield general insight into the species-wide architecture of this important trait.

None of the genes found here was involved in a transcriptomic study on drought response in beech saplings (Müller *et al.* 2017). However, most of the reliably annotated genes with or close to SNP loci significantly associated with drought phenotypes had putative homologs in other plant species

266 previously shown to be involved in drought or different environmental stress response (for citations
267 see Suppl. Table 2). This observation may be considered as post-hoc evidence that drought was
268 indeed the most likely stressor causing the observed phenotypic responses. It remained unclear
269 whether the remaining, not annotated genes had not yet been associated with drought before, or
270 whether we were just unable to make this link them due to the lack of (ecological) annotation and
271 standardised reporting. (Waldvogel *et al.* 2021) The involvement of in total 67 genes together with
272 the relatively flat effect size distribution suggested that drought resistance in *F. sylvatica* is a
273 moderately polygenic trait, which should respond well to artificial breeding attempts and natural
274 selection. However, given the relatively strict threshold criteria, it is likely that more yet undetected
275 loci contribute to the respective phenotypes. The low LD in beech predicts that an adaptation to
276 drought will not compromise genome-wide genetic diversity and thus adaptation potential to other
277 stressors. We achieved a high level of accuracy using genomic data to predict the drought phenotype
278 from individuals not used to identify drought associated SNP loci. However, due to the small sample
279 size, LDA might have resulted in overfitting (Hawkins 2004). We therefore also used a non-parametric
280 machine learning algorithm that has been shown to produce more robust results, especially for small
281 sample sizes (Horenko 2020).Both analyses confirmed that we mainly identified alleles widespread
282 throughout the sampled range and not locally specific. Besides, we confirmed a considerable level of
283 genetic variation in the sampled regions. The observation that trees with the highest predictive
284 values showed no loss of heterozygosity indicated that there is still adaptive potential for drought
285 adaptation in the species (Gienapp *et al.* 2017).With the SNP assay, we therefore created a tool that
286 can i) support the choice of seed trees for reforestations, ii) provide decision guidance for selective
287 logging and iii) monitor, whether natural selection on this quantitative trait is already acting in the
288 species. The current study can also serve as a starting point for molecular and physiological research
289 on how the identified loci or variants may, alone or in concert, confer resilience or tolerance to a
290 range of drought stress symptoms.

291 Material and Methods

292 *Sampling and phenotyping*

293 In August/early September 2019, we sampled leaf tissue of 402 *Fagus sylvatica* trees from 32
294 locations in Hessen/Germany (set 1, Figure 1), of which 300 were used for the (pool)GWAS analysis.
295 Forty three, plus additional 53 trees which were sampled in n August 2020, additional 52 trees from
296 four sites were sampled (set 2, Figure 1) made up the confirmation set. The coordinates and
297 characteristics of each site can be found in Suppl. Table 1. The sampling was performed in a strictly
298 pairwise design. The pairs consisted of one tree with heavy drought damage of the crown (lost or
299 rolled up, dried leaves) and one with an unaffected crown, respectively. This categorisation into least
300 and most damaged trees was taken compared to the other trees in the respective forest patch. The
301 pairs were *a priori* chosen such that the two trees were i) mutually the closest neighbours with
302 contrasting damage status (i.e. no other tree in the direct sight-line), ii) free from apparent
303 mechanical damage, fungal infestations or other signs of illness, similar iii) in tree height, iv) trunk
304 circumference, v) light availability, and vi) canopy closure. In addition, each pair was situated at least
305 30 m from the closest forest edge. For each tree of the chosen pairs, we recorded the exact position,
306 distance to the pair member and the estimated tree height (in 1 m increments), measured the trunk
307 circumference at 150 cm height above the ground (in 10 cm increments), and estimated the leaf loss
308 of the crown and the proportion of dried leaves (in 5% increments). We also recorded the estimated
309 distance (in 1 m resolution) and the specific identity of the two closest neighbour trees for each pair
310 member and calculated a competition index C as follows: $C = S_1/D_1 + S_2/D_2$, where S_1 and S_2 are the
311 trunk diameter at 150 cm and D_1 and D_2 the distances of the nearest and second nearest neighbour

312 tree of the same size or larger than the focal tree. Photographs from the crown and the trunk were
313 taken from the trees sampled in 2019.

314 From each tree, we sampled 5 to 10 fully developed leaves from low branches. The leaves sampled
315 from each tree were placed in paper bags. After returning from the field, they were dried at 50°C for
316 30-90 min and then kept on salt until they could be stored at -80°C.

317 *Climate and remote sensing data*

318 Monthly daily mean minimum and maximum temperature values and precipitation data were
319 obtained for the 1 x 1 km grid cells harbouring the sampling sites for the period between 1950 and
320 2019. Data on the accumulated potential evapotranspiration during the growth season was obtained
321 for the same grid cells. The data is publicly available from
322 https://opendata.dwd.de/climate_environment/CDC/grids_germany/monthly/.

323 Leaf area index (LAI) data for the above grid cells was obtained from Copernicus remote sensing
324 (www.copernicus.eu) for the period 2014-2019, considering only the month of August. To see
325 whether drought conditions influenced leaf coverage of the woods at the sampling sites, we
326 calculated the relative annual deviation of LAI from the 2014 value. We correlated it to the relative
327 deviation of the cumulated potential evatransporation over the growth season from 2014. The year
328 2014 was used as a baseline, because of the significant drought increase since then (Büntgen *et al.*
329 2021). Please note that the absolute level of LAI depends on the wood coverage, vegetation density
330 and species composition of each plot. Changes in LAI are thus not exclusively due to drought
331 damages in beech.

332 *DNA extraction, construction of GWAS pools and sequencing*

333 DNA was extracted from 12.5 mm^2 of a single leaf from each tree following the NucleoMag Plant Kit
334 (Macherey Nagel, Düren, Germany) protocol. We set up four DNA pools for poolGWAS by pooling
335 equal amounts of DNA from each individual: damaged individuals from the Southern part (dSouth),
336 healthy individuals from the South (hSouth), damaged North (dNorth) and healthy North (hNorth).
337 The Southern pools consisted of 100 individuals each, the Northern pools of 50 individuals each. The
338 pools were sent to Novogene (Cambridge, UK) for library construction and 150bp paired end
339 sequencing with 350bp insert size with 25Gb data for the northern and 38Gb data for the southern
340 samples. The 100 individuals used to construct the Northern pools were also individually re-
341 sequenced. The exact composition of the genomic pools can be found in Supplemental Table 1. All
342 sequence information can be found on the European Nucleotide Archive (ENA) under project
343 accession number *PRJEB24056.*

344 *Reference genome improvement*

345 We used an improved version of the recently published reference genome for the European beech
346 (Mishra *et al.* 2018). Contiguity was improved to chromosome level using Hi-C reads with the help of
347 the allhic software after excluding the probable organelle backbones from the earlier assembly that
348 was generated from the Illumina-corrected PacBio reads using Canu assembler (Mishra *et al.* 2021)
349 Access. No. PRJNA450822.

350 *Mapping and variant calling*

351 Reads of pools and individual resequencing were trimmed using the wrapper tool autotrim v0.6.1
352 (Waldvogel *et al.* 2018) that integrates trimmomatic (Bolger *et al.* 2014) for trimming and fastQC
353 (Andrews 2010) for quality control. The trimmed reads were then mapped on the latest chromosome
354 level build of the *F. sylvatica* genome using the BWA mem algorithm v.0.7.17 (Li & Durbin 2009). Low

355 quality reads were subsequently filtered and SNPs were initially called using samtools v.1.10 (Li *et al.*
356 2009). A principal component analysis (PCA) was conducted on unlinked single nucleotide
357 polymorphisms (SNPs) using the R package Factoextra v.1.0.7 (Kassambara & Mundt 2017).

358 *Pool GWAS and PLINK*

359 The PoPoolation pipeline 2_2012 (Kofler *et al.* 2011a; Kofler *et al.* 2011b) was used to call SNPs and
360 remove indels from the four pools. Allele frequencies for all SNPs with a coverage between 15x and
361 100x with a minimum allele count of three were estimated with the R library PoolSeq v. 0.35 (Taus *et*
362 *al.* 2017).

363 The statistical test to detect significant allele frequency differences among damaged and healthy
364 trees was the Cochran-Mantel-Haenszel test. With this test, a 2x2 table was created for each variable
365 position and region with two phenotypes (healthy and damaged). The read counts of each allele for
366 each phenotype were treated as the dependent variables. We controlled for false discovery rate
367 using the Benjamini-Hochberg correction R package *p.adjust*.

368 For the individual resequencing data we followed the GATK-pipeline 4.1.3.0 (DePristo *et al.* 2011). In
369 short, Picard tools v.2.20.8 was used to mark duplicates. GVCF files were created with
370 HaplotypeCaller and genotyped with GEnotypeGVCFs. Since we did not have a standard SNP set we
371 hard filtered SNPs with VariantFiltration QD<2.0, MQ<50.0, MQRankSum<12.5,
372 ReadPosRankSum<8.0, FS>80.0, SOR>4.0 and QUAL<10.0. This conservative SNP-set was used for
373 base recalibration before running the HaplotypeCaller pipeline a second round. Finally, the
374 genotyped vcf-files were filtered using vcftools with --maf 0.03 --max-missing 0.9 --minQ 25 --min-
375 meanDP 10 --max-meanDP 50 --minDP 10 --maxDP 50. The detailed pipeline can be found in Suppl.
376 Info 2.

377 To conduct the GWAS association on the above generated SNP set with phenotypes being either
378 damaged or healthy and to generate a principal component analysis on the SNP positions of the
379 individually resequenced trees, we used PLINK 1.9 (Purcell *et al.* 2007). The detailed workflow can be
380 found in Suppl. Info 2. We calculated a non-parametric ANOSIM on an inter-individual Euclidean
381 distance matrix based on the first ten principal components to infer whether the trees within
382 phenotype groups are overall genetically more similar than within groups (9,999 permutations;
383 (Hammer *et al.* 2001).

384 *Inference of Linkage Disequilibrium*

385 The expected length of segregating haplotypes in a species depends on the recombination rate and
386 their age. The former can be approximated by an estimate of linkage disequilibrium (LD. To
387 determine LD decay based on individually re-sequenced data we used the software LDkit v 1.0.0
388 (Tang *et al.* 2020), in 1kb and 100kb windows.

389 *Identification substitution type and gene function*

390 We inferred whether significantly differentiated SNPs within genes lead to a (non-) synonymous
391 amino acid substitution using tbg-tools v0.2 (https://github.com/Croxa/tbg-tools) (Schoennenbeck *et*
392 *al.* 2021). The protein sequences of the identified genes were used in a blastp search against all non-
393 redundant GenBank CDS translations, PDB, SwissProt, PIR, PRF to infer potential gene functions. Only
394 the best BLAST-hits were considered.

395 *Selection of SNP loci for SNPtype™ assay design*

For the design of SNPtype™ assays we used the web-based D3 assay design tool (Fludigm corp.). We aimed in first preference for the most significant SNPs of each genomic region identified by Pool-GWAS (80 loci). If this was technically impossible and the region harboured more than a single significant SNP, we opted for the second most significant SNP and so forth. This resulted finally in 76 suitable loci. The remaining 20 loci were recruited from the 20 most significant SNPs of the PLINK analysis that were not scored in the Pool-GWAS.

SNP genotyping procedure

For validation of drought susceptibility associated SNPs, we conducted SNP genotyping on 96.96 Dynamic Arrays (Fluidigm) with integrated fluidic circuits (Wang *et al.* 2009, 2009). (N=96) to validate the effictiveness of the identified SNPs in discriminating healthy from damaged trees. Prior to genotyping PCR, DNA extracts were normalised to approximately 5-10 ng/µl. They underwent a pre-amplification PCR (Specific Target Amplification, STA) according to the manufacturer's protocol to enrich target loci. PCR products were diluted 1:10 with DNA suspension buffer (TEKnova, PN T0221) before further use. Genotyping was performed according to the recommendations of manufacturer. Four additional PCR cycles were added to accommodate for samples of lower quality or including inhibitors (von Thaden, 2020). Fluorescent data were measured using the EP1 (Fluidigm) and analysed with the SNP Genotyping Analysis Software version 4.1.2 (Fluidigm). The automated scoring of the scatter plots was checked visually and if applicable, manually corrected.

Genomic prediction

To predict drought susceptibility from genotype data, we used a linear discriminant analysis (LDA) on 92 genotypes scored with the Fluidigm assay at 70 loci. Genotypes homozygous for the reference allele were scored as 0, heterozygous as 1 and homozygous alternate alleles as 2. We used the LDA option implemented in PAST v. 4.05. (Hammer, 2001).

We also used a non-parametric entropy-based Scalable Probabilistic Analysis framework (eSPA). This method allows simultaneous solution of feature selection and clustering problems, meaning that does not rely on a particular choice of user-defined parameters and has been shown to produce more robust results, especially for small sample sizes (Gerber2020, Horenko2020). Following the suggestion of the user manual, eSPA analysis was run 100 times with independent cross-validations of the Area Under the Curve (AUC) on the validation data.

Acknowledgments

There was no external funding for this study. We thank the SBiK-F Data- and Modelling Centre (Aidin Niamir) for support in obtaining climate and remote sensing data. CC acknowledges support from the Emergent AI Center funded by the Carl-Zeiss-Stiftung.

Additional information

Author contributions

Markus Pfenninger: Conceptualisation, sampling, data analysis, writing – original draft. Friederike Reuss, Angelika Kiebler: Laboratory support. Philipp Schönnenfeld, Cosima Caliendo, Susanne Gerber: Bioinformatics support. Berardino Cocchiararo: SNP-assay. Sabrina Reuter, Nico Blüthgen, Karsten Mody: Conceptualisation, sampling, data analysis. Miklós Bálint: Conceptualisation, data analysis. Bagdevi Mishra, Marco Thines: Bioinformatics support. Barbara Feldmeyer: Conceptualisation, labwork, data analysis. All authors read and approved the final version of the manuscript.

Author ORCIDs

Markus Pfenninger 0000-0002-1547-7245

Susanne Gerber 0000-0001-9513-0729

Berardino Cocchiararo 0000-0002-8427-7861

Karsten Mody 0000-0002-9251-0803

Marco Thines 0000-0002-9251-0803

Barbara Feldmeyer 0000-0002-0413-7245

Data availability

Sequencing data have been deposited at ENA under project code PRJEB41889.

The genome assembly including the annotation is available under the Access. No. PRJNA450822.

References

Andrews S (2010) FastQC: a quality control tool for high throughput sequence data. Babraham Bioinformatics, Babraham Institute, Cambridge, United Kingdom.

Aranda I, Cano FJ, Gascó A*, et al.* (2015) Variation in photosynthetic performance and hydraulic architecture across European beech (*Fagus sylvatica* L.) populations supports the case for local adaptation to water stress. *Tree Physiology* **35**, 34-46.

Bastide H, Betancourt A, Nolte V*, et al.* (2013) A genome-wide, fine-scale map of natural pigmentation variation in Drosophila melanogaster. *PLoS Genetics* **9**, e1003534.

Baumbach L, Niamir A, Hickler T, Yousefpour R (2019) Regional adaptation of European beech (*Fagus sylvatica*) to drought in Central European conditions considering environmental suitability and economic implications. *Regional Environmental Change* **19**, 1159-1174.

Belmonte J, Alarcón M, Avila A, Scialabba E, Pino D (2008) Long-range transport of beech (*Fagus sylvatica* L.) pollen to Catalonia (north-eastern Spain). *International Journal Of Biometeorology* **52**, 675-687.

Bolger AM, Lohse M, Usadel B (2014) Trimmomatic: a flexible trimmer for Illumina sequence data. *Bioinformatics* **30**, 2114-2120.

Bolte A, Czajkowski T, Cocozza C*, et al.* (2016) Desiccation and mortality dynamics in seedlings of different European beech (*Fagus sylvatica* L.) populations under extreme drought conditions. *Frontiers in plant science* **7**, 751.

Bošeľa M, Sedmák R, Marušák R*, et al.* (2014) Evaluating similarity of radial increments around tree stem circumference of European beech and Norway spruce from Central Europe. *Geochronometria* **41**, 136-146.

Bressem U (2008) Komplexe Erkrankungen an Buche. Complex diseases in beech. *Ergebnisse angewandter Forschung zur Buche* **3**, 87.

Brunet J, Fritz Ö, Richnau G (2010) Biodiversity in European beech forests-a review with recommendations for sustainable forest management. *Ecological Bulletins*, 77-94.

Büntgen U, Urban O, Krusic PJ*, et al.* (2021) Recent European drought extremes beyond Common Era background variability. *Nature Geoscience*, 1-7.

Carrière SD, Ruffault J, Cakpo CB*, et al.* (2020) Intra-specific variability in deep water extraction between trees growing on a Mediterranean karst. *Journal of Hydrology* **590**, 125428.

Choat B, Brodribb TJ, Brodersen CR*, et al.* (2018) Triggers of tree mortality under drought. *Nature* **558**, 531-539.

Christensen JH, Hewitson B, Busuioc A*, et al.* (2007) Regional climate projections. In: *Climate Change, 2007: The Physical Science Basis. Contribution of Working group I to the Fourth Assessment Report of the Intergovernmental Panel on Climate Change, University Press, Cambridge, Chapter 11*, pp. 847-940.

Cocozza C, De Miguel M, Pšidová E*, et al.* (2016) Variation in ecophysiological traits and drought tolerance of beech (*Fagus sylvatica* L.) seedlings from different populations. *Frontiers in Plant Science* **7**, 886.

Czajkowski T, Bolte A (2006) Frosttoleranz deutscher und polnischer Herkünfte der Buche (*Fagus sylvatica* L.) und ihre Beeinflussung durch Trockenheit. *Archiv für Forstwesen und Landschaftsökologie* **40**, 119-126.

DePristo MA, Banks E, Poplin R*, et al.* (2011) A framework for variation discovery and genotyping using next-generation DNA sequencing data. *Nature Genetics* **43**, 491.

Dorow WH, Blick T, Kopelke J-P (2010) Zoologische Forschung in hessischen Naturwaldreservaten–Exemplarische Ergebnisse und Perspektiven. *Forstarchiv* **81**, 61-68.

Elsasser P, Meyerhoff J, Weller P (2016) An updated bibliography and database on forest ecosystem service valuation studies in Austria, Germany and Switzerland. Thünen Working Paper.

Endler L, Betancourt AJ, Nolte V, Schlötterer C (2016) Reconciling differences in pool-GWAS between populations: a case study of female abdominal pigmentation in *Drosophila melanogaster*. *Genetics* **202**, 843-855.

Etzold S, Ziemińska K, Rohner B*, et al.* (2019) One century of forest monitoring data in Switzerland reveals species-and site-specific trends of climate-induced tree mortality. *Frontiers in Plant Science* **10**, 307.

Gárate-Escamilla H, Hampe A, Vizcaíno-Palomar N, Robson TM, Benito Garzón M (2019) Range-wide variation in local adaptation and phenotypic plasticity of fitness-related traits in *Fagus sylvatica* and their implications under climate change. *Global Ecology and Biogeography* **28**, 1336-1350.

Gerber S, Pospisil L, Navandar M, Horenko I (2020). Low-cost scalable discretization, prediction, and feature selection for complex systems. *Science Advances*, **6**, eaaw0961.

Gienapp P, Fior S, Guillaume F*, et al.* (2017) Genomic quantitative genetics to study evolution in the wild. *Trends in Ecology & Evolution* **32**, 897-908.

Harris K, Nielsen R (2013) Inferring demographic history from a spectrum of shared haplotype lengths. *PLoS Genet* **9**, e1003521.

Harter DE, Nagy L, Backhaus S*, et al.* (2015) A comparison of genetic diversity and phenotypic plasticity among European beech (*Fagus sylvatica* L.) populations from Bulgaria and Germany under drought and temperature manipulation. *International Journal of Plant Sciences* **176**, 232-244.

Hawkins DM (2004) The problem of overfitting. *Journal of chemical information and computer sciences* **44**, 1-12.

Hoban S, Kelley JL, Lotterhos KE*, et al.* (2016) Finding the genomic basis of local adaptation: pitfalls, practical solutions, and future directions. *The American Naturalist* **188**, 379-397.

Horenko I (2020) On a Scalable Entropic Breaching of the Overfitting Barrier for Small Data Problems in Machine Learning. *Neural Computation* **32**, 1563-1579.

Kassambara A, Mundt F (2017) Factoextra: extract and visualize the results of multivariate data analyses. *R package version* **1**, 337-354.

Kofler R, Orozco-terWengel P, De Maio N*, et al.* (2011a) PoPoolation: A Toolbox for Population Genetic Analysis of Next Generation Sequencing Data from Pooled Individuals. *PLoS One* **6**, e15925.

Kofler R, Pandey RV, Schlötterer C (2011b) PoPoolation2: identifying differentiation between populations using sequencing of pooled DNA samples (Pool-Seq). *Bioinformatics* **27**, 3435-3436.

Kreyling J, Thiel D, Nagy L*, et al.* (2012) Late frost sensitivity of juvenile *Fagus sylvatica* L. differs between southern Germany and Bulgaria and depends on preceding air temperature. *European Journal of Forest Research* **131**, 717-725.

Lander TA, Klein EK, Roig A, Oddou-Muratorio S (2021) Weak founder effects but significant spatial genetic imprint of recent contraction and expansion of European beech populations. *Heredity* **126**, 491-504.

Li H, Durbin R (2009) Fast and accurate short read alignment with Burrows-Wheeler Transform. *Bioinformatics* **25**, 1754-1760.

Li H, Handsaker B, Wysoker A*, et al.* (2009) The Sequence alignment/map (SAM) format and SAMtools. . *Bioinformatics* **25**, 2078-2079.

Magri D, Vendramin GG, Comps B*, et al.* (2006) A new scenario for the Quaternary history of European beech populations: palaeobotanical evidence and genetic consequences. *New Phytologist* **171**, 199-221.

Mishra B, Gupta DK, Pfenninger M*, et al.* (2018) A reference genome of the European beech (*Fagus sylvatica* L.). *Gigascience* **7**, giy063.

Mishra B, Ulaszewski B, Meger J*, et al.* (2021) A chromosome-level genome assembly of the European Beech (*Fagus sylvatica*) reveals anomalies for organelle DNA integration, repeat content and distribution of SNPs. *bioRxiv https://doi.org/10.1101/2021.03.22.436437*.

Müller M, Seifert S, Lübbe T, Leuschner C, Finkeldey R (2017) De novo transcriptome assembly and analysis of differential gene expression in response to drought in European beech. *PLoS One* **12**, e0184167.

Paaby A, Rockman M (2014) Cryptic genetic variation: evolution's hidden substrate. *Nature Reviews Genetics* **15**, 247–258.

Paar U, Dammann I (2019) Waldzustandsbericht Hessen 2019 (ed. Hessisches Ministerium für Umwelt K, Landwirtschft und Verbraucherschutz), Wiesbaden.

Pluess AR, Frank A, Heiri C*, et al.* (2016) Genome–environment association study suggests local adaptation to climate at the regional scale in *Fagus sylvatica*. *New Phytologist* **210**, 589-601.

Pretzsch H, Schütze G, Uhl E (2013) Resistance of European tree species to drought stress in mixed versus pure forests: evidence of stress release by inter-specific facilitation. *Plant Biology* **15**, 483-495.

Purcell S, Neale B, Todd-Brown K*, et al.* (2007) PLINK: a tool set for whole-genome association and population-based linkage analyses. *The American Journal of Human Genetics* **81**, 559-575.

Rajendra K, Seifert S, Prinz K, Gailing O, Finkeldey R (2014) Subtle human impacts on neutral genetic diversity and spatial patterns of genetic variation in European beech (*Fagus sylvatica*). *Forest Ecology and Management* **319**, 138-149.

Schoennenbeck P, Schell T, Gerber S, Pfenninger M (2021) tbg-a new file format for genomic data. *bioRxiv https://doi.org/10.1101/2021.03.15.435393*.

Schuldt B, Buras A, Arend M*, et al.* (2020a) A first assessment of the impact of the extreme 2018 summer drought on Central European forests. *Basic and Applied Ecology* **45**, 86-103.

Schuldt B, Buras A, Arend M*, et al.* (2020b) A first assessment of the impact of the extreme 2018 summer drought on Central European forests. *Basic and Applied Ecology*.

Stocks JJ, Metheringham CL, Plumb WJ*, et al.* (2019) Genomic basis of European ash tree resistance to ash dieback fungus. *Nature Ecology & Evolution* **3**, 1686-1696.

Sutmöller J, Spellmann H, Fiebiger C, Albert M (2008) Der Klimawandel und seine Auswirkungen auf die Buchenwälder in Deutschland The effects of climate change on beech forests in Germany. *Ergeb. Angew. Forsch. Buche* **3**, 135.

Tang Y, Li Z, Wang C*, et al.* (2020) LDkit: a parallel computing toolkit for linkage disequilibrium analysis. *BMC Bioinformatics* **21**, 1-8.

Taus T, Futschik A, Schlötterer C (2017) Quantifying selection with pool-seq time series data. *Molecular Biology and Evolution* **34**, 3023-3034.

Thünen_Institute (2020) Clusterstatistik Forst & Holz.

Trenberth KE, Dai A, Van Der Schrier G*, et al.* (2014) Global warming and changes in drought. *Nature Climate Change* **4**, 17-22.

Waldvogel AM, Feldmeyer B, Rolshausen G*, et al.* (2020) Evolutionary genomics can improve prediction of species' responses to climate change. *Evolution Letters* **4**, 4-18.

Waldvogel A-M, Schreiber D, Pfenninger M, Feldmeyer B (2021) Climate Change Genomics Calls for Standardized Data Reporting. *Coping with Climate Change: A Genomic Perspective on Thermal Adaptation*.

Waldvogel AM, Wieser A, Schell T*, et al.* (2018) The genomic footprint of climate adaptation in *Chironomus riparius*. *Molecular Ecology* **27**, 1439-1456.

Wang J, Lin M, Crenshaw A, *et al.* (2009) High-throughput single nucleotide polymorphism genotyping using nanofluidic Dynamic Arrays. *BMC Genomics* **10**, 561.

Wellenreuther M, Hansson B (2016) Detecting polygenic evolution: problems, pitfalls, and promises. *Trends in Genetics* **32**, 155-164.

Figures

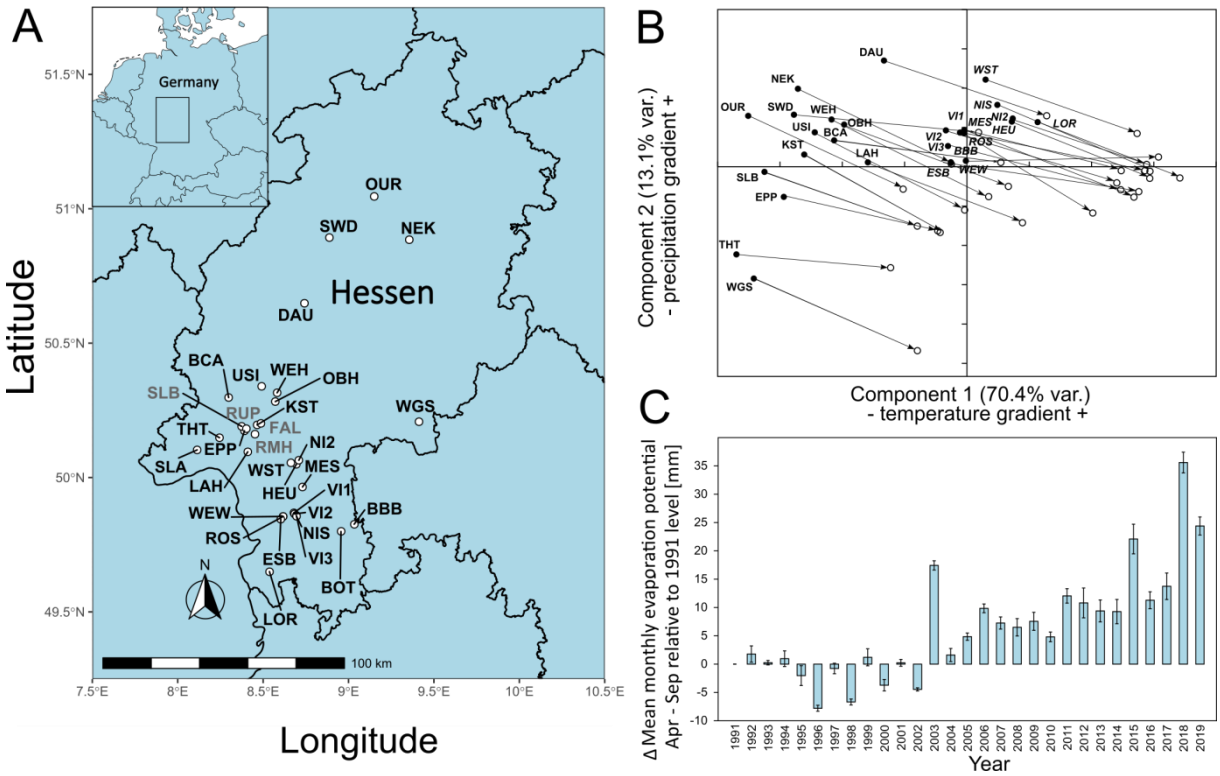

Figure 1. A) Locations of sampling sites in Hessen, Germany. For abbreviations see Suppl. Table 1. The sites where confirmation individuals were sampled are designated in grey.B) Principal Component Analysis of monthly climate data 1950-2019, C) Development of main growth period drought indicator from 1991-2019. Shown is the difference mean monthly evaporation potential in mm from April to September relative to the 1991 level. Climate and drought data obtained from https://opendata.dwd.de/climate_environment/CDC/grids_germany/monthly/.

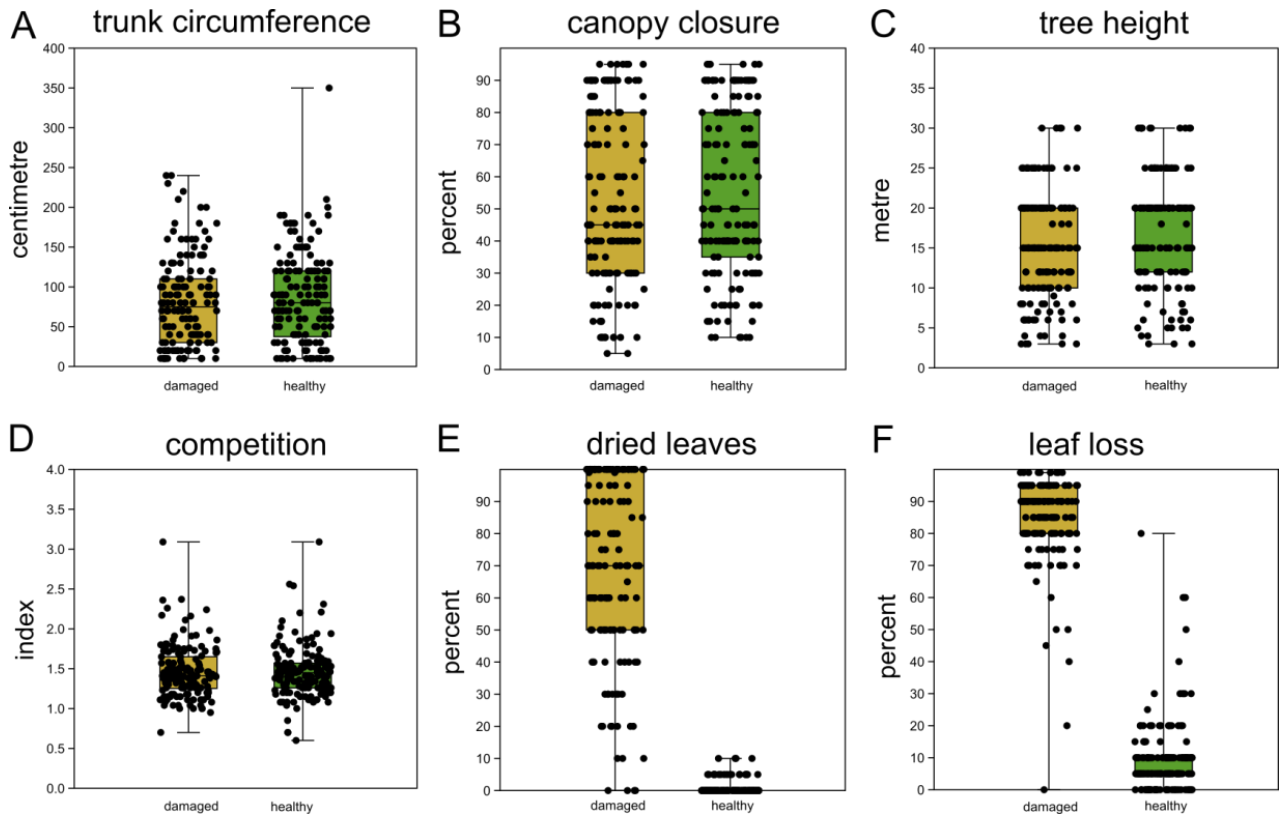

Figure 2. Comparison of sampled beech pairs. A) trunk circumference, B) canopy closure, C) tree height, D) competition index, E) dried leaves and F) leaf loss. Box-plots with indicated means, the boxes represent one standard deviation, the whiskers are the 95% confidence intervals. Damaged trees in ochre, healthy trees in green. Except for E and F, the difference of means among damaged and healthy trees is insignificant between the groups.

A

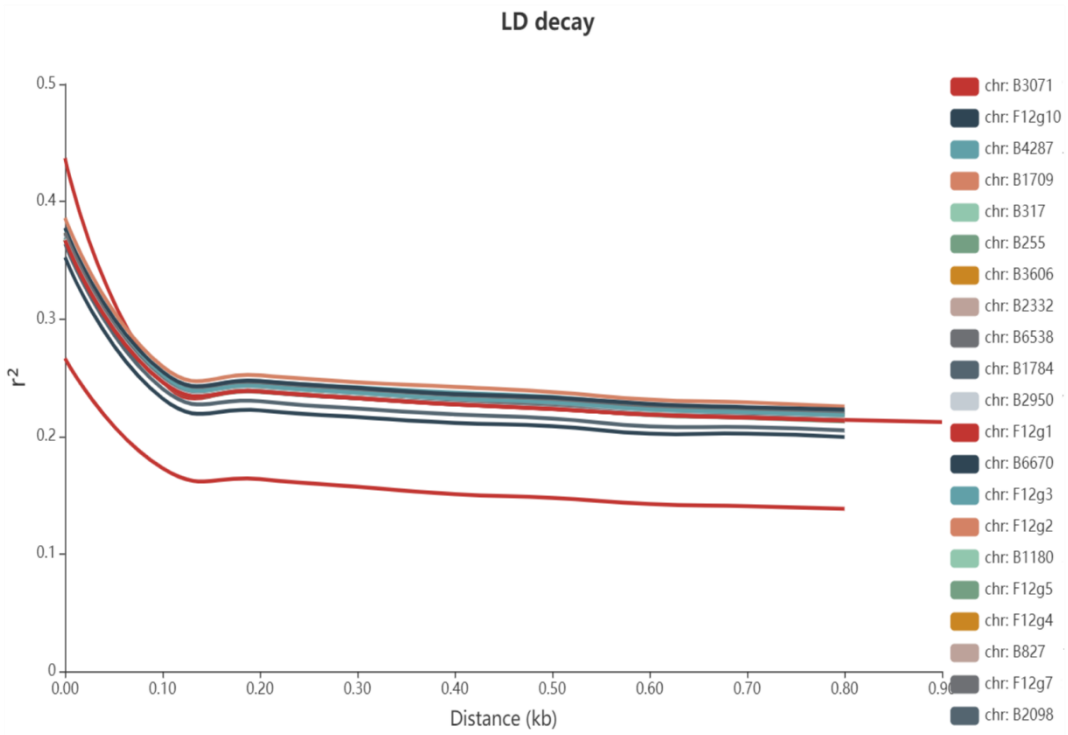

B

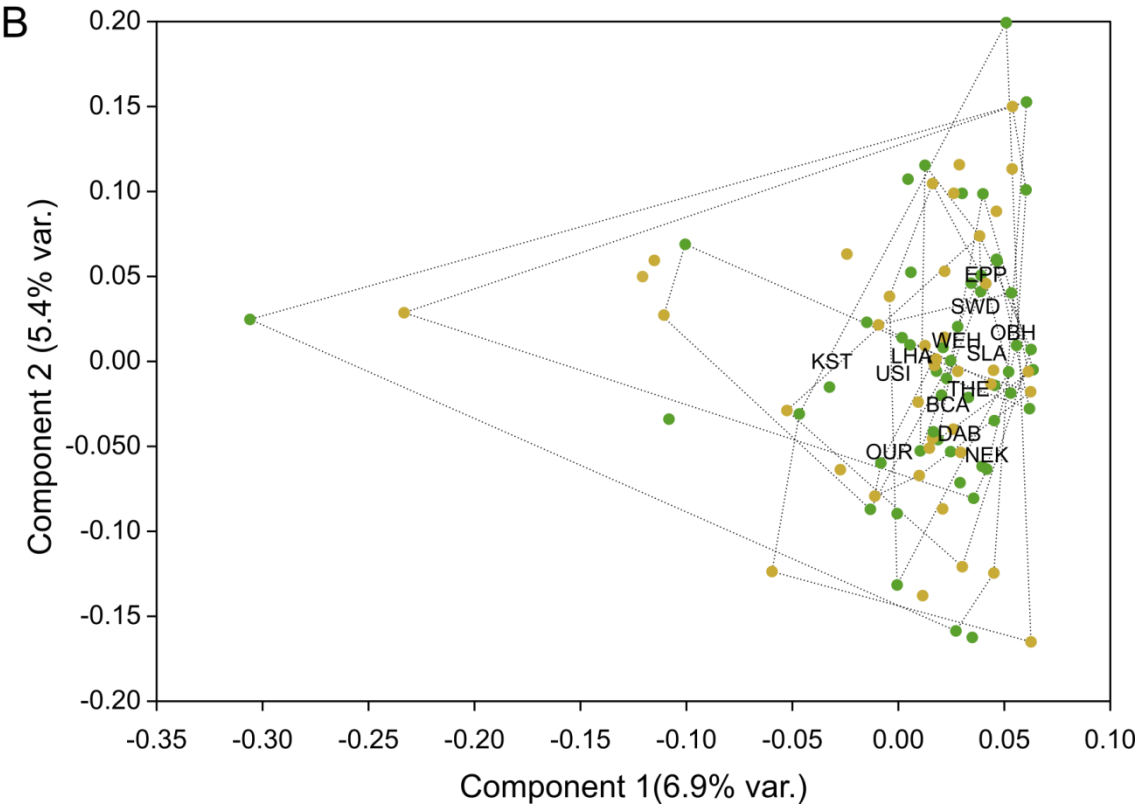

Figure 3. Genome wide linkage disequilibrium and principal component analysis on genome-wide SNP data. A) Decay of genome wide linkage disequilibrium (LD), measured as r^2 on allele frequencies gained from individual resequencing, with distance from focal SNP in base pairs. B) Plot of the first two principal component axes of LD pruned SNP data from individually sequenced beech individuals

613 from the North population. Healthy trees are indicated by a green dot, damaged ones by ochre.
614 Individuals sampled from the same site are grouped by convex hulls, limited with dotted lines.

615

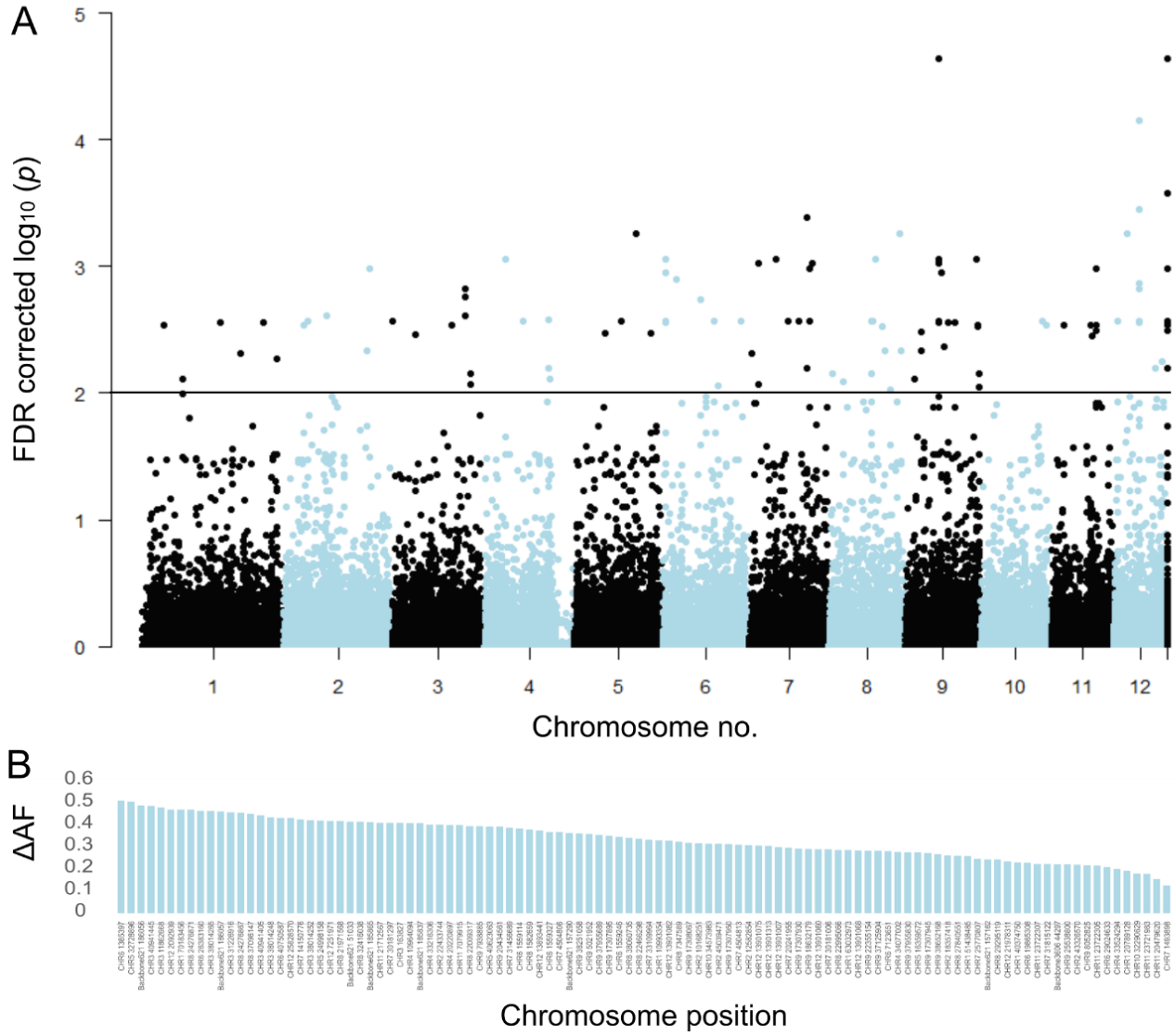

Figure 4. Significantly associated drought phenotype associated SNP marker. A) Manhattan plot of false discovery rate (FDR) corrected –log10 probability values from CMH test. The black horizontal line indicates the chosen significance threshold. SNPs on different chromosomes alternate in colour (black and blue). B) Mean allele frequency difference at significantly associated SNP loci between healthy and damaged phenotypes. The loci are ordered according to amount of change.

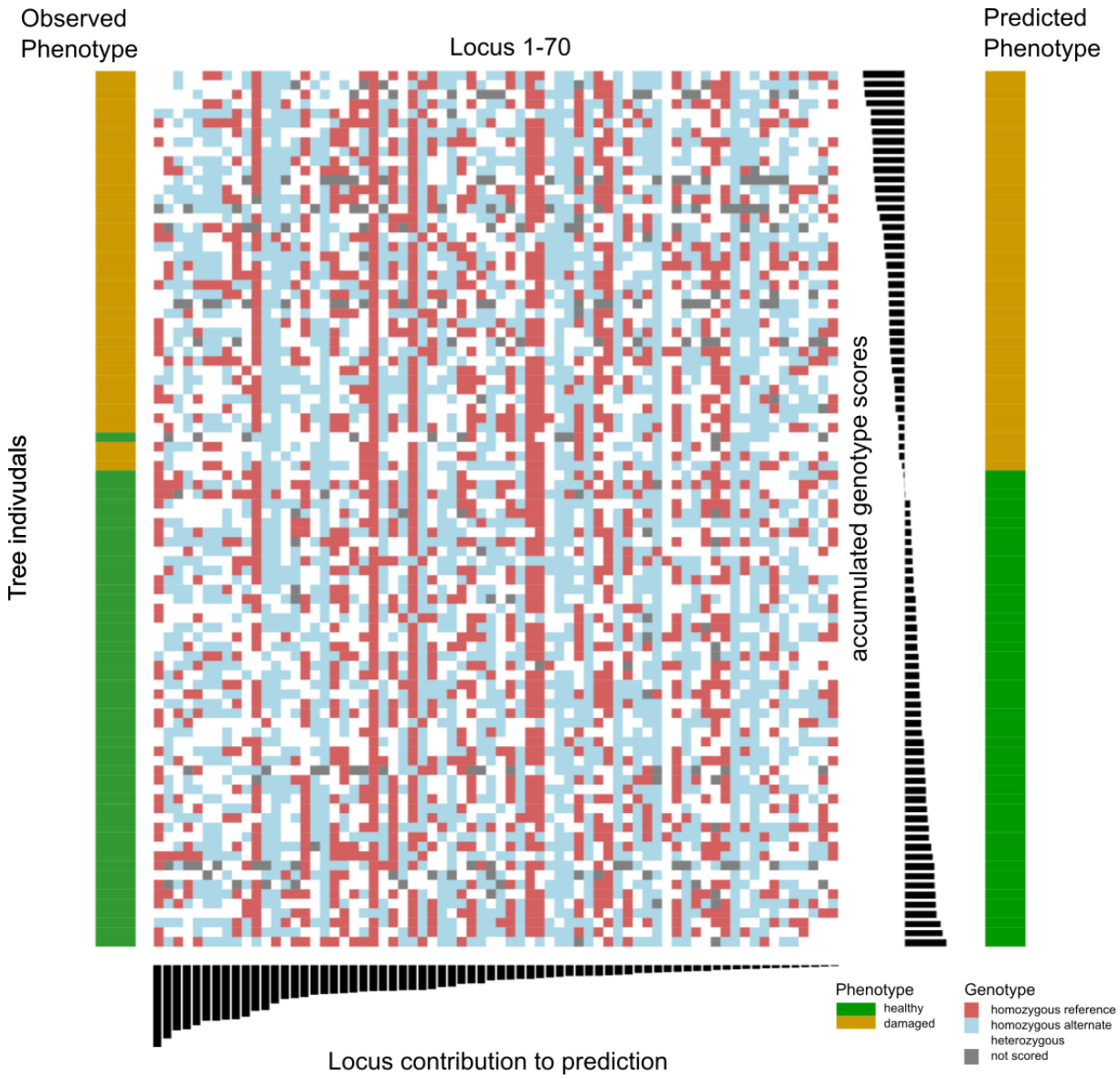

Figure 5. Combined results of SNP assay and discriminant analyses. The centre of the figure depicts the genotypogram of the SNP assay. Each column represents one of 70 loci, each row one of 92 beech individuals. The scored genotypes are colour-coded, with red squares = homozygous reference allele, light blue = homozygous alternate allele, white = heterozygous SNP, grey squares = locus could not be scored in the respective individual. The left bar indicates the observed phenotype for each tree individual with ochre rectangles for damaged, and green for healthy trees. Below the genotypogram, the relative contribution of each locus to the predictive model of the discriminant analysis is indicated, ordered from high to low. On the right side, first the genotype model scores for each individual are given, with the according predicted phenotype (ochre = damaged; green = healthy).

Tables

Table 1. Genes with significantly associated SNPs. Given are the chromosome number (CHR), nucleotide position (position), the gene ID for *Fagus sylvatica* (gene), the UniProt ID of the closest match (UniProt ID), the name of the gene (name), the nucleotide base in the reference (ref DNA base), and the alternate base (alt DNA base), if applicable, the amino acid of the reference (ref AA) and the alternate base (non-synonymous change), functional change (effect) and the phenotype associated with the alternate base.

CHR	position	gene	UniProt ID	name	ref DNA base	alt DNA base	ref AA	non-synoynmous change	effect	phenotype assoc. with alt base
1	40374762	1.g3851.t1	none		A	G	C	R	SH side chain > positive charge	healthy
10	32290645	10.g3914.t1	none		C	T	F	-	-	
11	20479628	11.g2467.t1	EXOS5_ORYSJ	Exosome complex exonuclease RRP46 homolog	T	C	T	A	polar > hydrophobic	damaged
11	23722307	11.g2832.t1	PCN_ARATH	WD repeat-containing protein PCN	A	G	I	V	hydrophobic > hydrophobic	damaged
12	13901034	12.g1695.t1	F4I5S1_ARATH	PB1 domain-containing protein tyrosine kinase	C	A	P	Q	hydrophobic > polar	damaged
	13901063				C	T	Q	stop	termination	damaged
	13901082				A	T	H	L	positive charge > hydrophobic	damaged
	13901094				T	A	I	N	hydrophobic > polar	damaged
2	43326571	2.g4736.t1	none		G	A	R	C	positive charge > SH side chain	damaged
3	31226940	3.g3590.t1	none		C	T	Q	stop	termination	healthy
4	34077017	4.g3980.t1	CKX1_ARATH	Cytokinin dehydrogenase 1	C	A	G	C	no side chain > SH side chain	damaged
5	16359587	5.g1807.t1	GDI2_ARATH	Guanosine nucleotide diphosphate dissociation inhibitor 2	T	C	P	-	-	
6	19865311	6.g2227.t1	NDUS7_ARATH	NADH dehydrogenase [ubiquinone] iron-sulfur protein 7, mitochondrial	T	C	D	-	-	
6	26383172	6.g2921.t1	none		T	C	A	-	-	
7	1493904	7.g177.t1	TLP10_ARATH	Tubby-like F-box protein 10	C	T	G	-	-	
7	20242023	7.g2350.t1	PRK4_ARATH	Pollen receptor-like kinase 4	A	G	P	-	-	
7	4504799	7.g1655			C	T	W	stop	termination	damaged

7	31456694	7.g3617.t1	LSH4_ARATH	Protein LIGHT-DEPENDENT SHORT HYPOCOTYLS 4	G	T	R	-	-	
7	33110000	7.g3816.t1	none		G	A	L	-	-	
7	4504813	7.g552.t1	none		G	A	G	-	-	
	4504831				C	T	L	-	-	
8	29295139	8.g3494.t1	VATC_ARATH	V-type proton ATPase subunit C	G	A	G	-	-	
9	25538827	9.g3080.t1	PPA14_ARATH	Probable inactive purple acid phosphatase 14	G	C	K	N	positive charge > polar	damaged
9	37955715	9.g4504.t1	TBL33_ARATH	Protein trichome birefringence-like 33	G	C	M	I	hydrophobic > hydrophobic	damaged